ZEROBUILD JOURNAL

Araştırma Makalesi

Buker ve ark. 04:01 (2026) 41-54

PCM ile Evsel Sıcak Su Tankı Termal Performans Değerlendirmesi ve HAD Analizleri ile Enerji Verimliliği İyileştirmesi

Mahmut Sami BÜKER[1], Veli Can GÜRAN[2], Ahmet Emre ONAY[2], Halil İbrahim DAĞ[4]

[1]Necmettin Erbakan University, Konya, Turkiye
[2]Innorma R&D Inc., Konya, Turkiye
[3]SOLIMPEKS Solar, Konya, Turkiye
Sorumlu Yazar: msbuker@erbakan.edu.tr

Öne Çıkanlar:

- Geliştirilmiş Enerji Depolama: 300 L kapasiteli ev tipi bir sıcak su tankına 3 kg parafin bazlı farklı FDM'lerin (MP46, RT47 ve MP52) entegrasyonu, şarj süresini önemli ölçüde etkilemeden, kullanılabilir sıcak su miktarını 20 L artırmıştır (RT47).
- Isı Kaybının Azaltılması: MP52 FDM'li sıcak su tankı, bekleme süresince daha düşük ısı kayıpları sergileyerek (79.95W), gelişmiş termal stabilite ve enerji verimliliği sağlamıştır.
- Sürdürülebilirlik Potansiyeli: Evsel sıcak su sistemlerine FDM entegrasyonu, enerji tasarrufuna katkıda bulunarak, sürdürülebilir, kullanıcı odaklı sıcak su çözümlerinin geliştirilmesini desteklemiştir.

Geliş Tarihi: 30.12.2025 Kabul Tarihi: 18.01.2026 Doi: 10.5281/zenodo.18362176

Amaç:
Günümüzde sürdürülebilir ısıtma uygulamalarında enerji verimliliğinin artırılması kritik önem taşımaktadır. Bina sektöründe kullanım sıcak suyu (KSS) tüketiminin toplam enerji tüketiminin yaklaşık %30'unu oluşturması nedeniyle, sıcak su depolama tanklarının verimliliğinin artırılması önemli bir enerji tasarrufu potansiyeli sunmaktadır. Bu çalışma, 300 L hacmindeki bir kullanım sıcak suyu tankına entegre edilen 3 kg parafin bazlı Faz Değişim Malzemesinin (FDM), şarj, deşarj ve bekleme sürelerindeki ısıl performans üzerindeki etkisini incelemeyi amaçlamaktadır.
Materyal ve Metod:
FDM entegreli ve konvansiyonel tanklar için şarj, deşarj ve ısı kaybı analizleri Hesaplamalı Akışkanlar Dinamiği (HAD) yöntemi kullanılarak gerçekleştirilmiştir. Deneysel bulgular da değerlendirilerek sayısal model doğrulanmıştır. Isı kaybı analizleri TS EN 12897+A1:2020-03 standardına uygun olarak yapılmış ve FDM'li ve FDM'siz tankların 180 dakikalık bekleme süresi sonundaki performansı karşılaştırılmıştır.
Sonuç:
Yapılan analizler, FDM'li sıcak su depolama tanklarında genel performansı belirgin şekilde iyileştirdiğini göstermektedir. Şarj süresinde FDM'lerin etkisi sınırlı olup, konvansiyonel tank 100 dakikada 50 °C'ye ulaşırken FDM'li tankların 105 dakika ile benzer sonuç vermesi, şarj sürecinin olumsuz etkilenmediğini ortaya koymuştur. Deşarj aşamasında ise FDM'ler önemli bir avantaj sağlayarak, RT47 için 16.40 dk, MP46 için 16.20 dk ve MP52 için 15.30 dk boyunca sıcak su temini sunmuş; bu değerler konvansiyonel tanka göre (14.10 dk) yaklaşık 2.5 dakika (~20 L) daha uzun kullanım süresi anlamına gelmiştir. Ayrıca, 55 °C'de 180 dakikalık bekleme süresinde konvansiyonel tankın 86.9 W olan ısı kaybı FDM'li tanklarda 79.95–82.3 W aralığına düşmüştür.
Anahtar Kelimeler: Faz değiştiren malzeme; termal enerji depolama; kullanım sıcak suyu; enerji verimliliği; hesaplamalı akışkanlar dinamiği.

ZEROBUILD JOURNAL

Research Article

Buker et al. 04:01 (2026) 41-54

Thermal Performance Assessment of Domestic Hot Water Tanks with PCM and Energy Efficiency Improvement Through CFD Analyses

Mahmut Sami BÜKER[1], Veli Can GÜRAN[2], Ahmet Emre ONAY[2], Halil İbrahim DAĞ[4]

[1]Necmettin Erbakan University, Konya, Turkiye
[2]Innorma R&D Inc., Konya, Turkiye
[3]SOLIMPEKS Solar, Konya, Turkiye
Sorumlu Yazar: msbuker@erbakan.edu.tr

Highlights:

- Enhanced Energy Storage: Integrating 3 kg of different paraffin-based PCMs (MP46, RT47 and MP52) into a 300 L capacity domestic hot water tanks increased the usable hot water volume by 20 L without significantly affecting charging time (RT47).
- Reduced Heat Loss: The MP52 PCM-enhanced hot water tank exhibits lower heat loss (79.95 W) in standby mode, resulting in improved thermal stability and energy efficiency.
- Sustainability Potential: Integrating PCMs into domestic hot water systems has contributed to energy savings and supporting the development of sustainable, user-oriented hot water solutions.

Received: 15.12.2025 Accepted: 10.01.2026 Doi: 10.5281/zenodo.18362176

Abstract: Energy efficiency has become increasingly critical in domestic hot water tank (DHWT) systems, as DHWT use accounts for approximately 30% of total energy consumption in buildings. Phase Change Material (PCM) integrated systems offer significant potential for improving thermal performance compared to conventional water-based storage. In this study, the charging, discharging, and heat loss behaviour of PCM-integrated DHWT were evaluated using Computational Fluid Dynamics (CFD). The results showed that adding 3 kg of paraffin-based PCM to a 300 L DHWT increased the usable hot water volume by at least 10% without significantly affecting the charging time. While the conventional tank provided usable hot water for 14.10 minutes, PCM integration extended this time by approximately 2 minutes due to the latent heat released during solidification. A heat loss analysis conducted according to the TS EN 12897+A1:2020-03 standard revealed that the conventional system showed a heat loss of 86.9 W at 55 °C, while the MP52 integrated tank reduced this value to 79.95 W after a 180-minute retention time. These findings demonstrate that combining sensible and latent heat storage reduces thermal losses, improves discharge performance, and contributes to overall energy savings. The study also offers recommendations for the future optimization of PCM-enhanced hot water systems, emphasizing improved control strategies to increase efficiency, particularly in material selection, PCM deployment, and next-generation hot water storage designs.

Keywords: Phase change material; thermal energy storage; domestic hot water, energy efficiency; computational fluid dynamics

1. Introduction

Increasing energy efficiency in buildings has made the optimization of heating and DHWT systems a key focus in building energy efficiency studies and sustainability strategies in recent years. The European Green Deal, which aims to achieve carbon neutrality by 2050, highlights the development of innovative and highly efficient solutions to reduce energy consumption in buildings. In this context, regulations and directives designed to enhance building energy performance, such as the Energy Performance of Buildings Directive (EPBD), encourage the design and use of energy efficient and low carbon DHWT systems. DHWT systems are particularly critical for energy efficiency, accounting for approximately 30 % of total building energy consumption, making them a focal point in sustainable building design [1, 2].

In addition to the conventional sensible heat storage methods, use of PCMs as heat storage medium offers significant advantages due to their ability to store a higher amount of energy [3]. PCMs store a considerable amount of latent heat during phase change, eventually increasing the overall energy storage capacity of the system [4]. This mechanism is particularly effective in extending the storage duration and increasing the amount of hot water available from the tank, allowing for faster response to user demand and significantly improving system energy efficiency.

Various studies in the literature have examined the use of PCMs in DHWTs contained in different geometries and application scenarios. These studies have analysed mainly the effects of PCM location in the tank, quantity, and container geometry on thermal energy storage performance. For example, in vertical mantle DHWTs, positioning paraffin capsules 400 mm above the bottom of the tank enabled the maximum hot water volume (639 L) to be achieved. In contrast, placing the capsules directly at the bottom of the tank (0 mm) reduced the obtainable hot water volume to 619 L. The data indicate a notable increase in hot water volume up to 400 mm, while exceeding 600 mm led to a decrease in the amount of hot water obtained [10].

Similarly, another study on vertical tanks determined that the optimum 32.5 kg PCM quantity was 13 paraffin capsules, which increased hot water output by approximately 20 % [5]. For horizontal mantle DHWTs, four 1 L paraffin tubes extended the discharge duration by 17 minutes and increased the amount of hot water obtained from the tank [6]. These results demonstrate that PCM location and quantity directly and measurably affect the thermal performance of the DHWT.

Another critical factor influencing DHWT performance is heat loss during standby periods. Thermal bridges at tank connections and insufficient or uneven insulation can negatively impact the preservation of stored energy, significantly reducing system efficiency. Therefore, minimizing heat loss is a fundamental design consideration to both enhance energy efficiency and maximize the effectiveness of PCM-integrated thermal energy storage systems [7].

This hybrid sensible-latent heat storage is also promising concept for renewable energy integration. A study on the energy and exergy flow analysis of primary energy sources has shown that solar collector systems provide the highest total energy and exergy efficiency among existing heating options [8]. They observed that energy efficiency ranges from 24.1% to 46.2% for Izmir and 22.4% to 40.3% for Paris under different scenarios. This finding indicates that integrating PCM-enhanced hot water storage tanks with solar collectors has an important potential for increasing energy efficiency in buildings. Furthermore, since the DHWT can be directly fed by solar collectors, the system reduces dependence on fossil fuel-based heating and consequently contributes to lowering total carbon emissions.

In a preliminary study, charging, discharging, and heat loss analyses were conducted. The results showed that the use of PCM in DHWTs increased the amount of hot water by 20 L compared to DHWTs without PCM. It also extended the hot water discharging time by approximately 2.5 minutes [9].

This study investigates the thermal performance of a 300 L DHWT with a vertical cylindrical configuration, comparing conventional operation with a PCM-integrated design. Unlike many previous studies that primarily focus on large PCM masses (typically 10–40 kg) or non-commercial and idealised tank geometries, the present work evaluates the integration of only 3 kg of paraffin-based PCM into a commercially available coil-type storage tank. The key novelty of this study lies in demonstrating that even a relatively small amount of PCM, when appropriately positioned within a tank configuration, can yield a measurable enhancement in thermal performance. This approach provides a more practical and industry-relevant assessment of PCM integration, addressing the gap between laboratory-scale investigations and real-world DHWT applications.

A validated three-dimensional CFD model was developed for the tank, and charge, discharge, and heat loss scenarios were analysed separately. During the charge analyses, temperature distributions and thermal response times were evaluated under constant inlet temperature and flow rate conditions to understand the tank's dynamic behaviour. During the discharge analyses, the temporal variation of the usable DHWT volume and outlet temperature was monitored. Heat loss analyses were conducted according to the TS EN 12897+A1 standard to assess thermal stability and energy savings during the specified holding period.

In addition to assessing energy storage capacity, the study also examines the impact of PCM integration on charge and discharging times, standby heat losses, and DHWT availability. The results provide a comparison between conventional and PCM-integrated tanks and highlight the performance advantages achieved by adding a small PCM volume. These features distinguish the current study from previous research.

2. Materials and Methods

2.1 System Description

In this study, a 3D model of a conventional 300 L DHWT in a vertical cylindrical geometry was realised (Figure 1). The tank has two separate coils positioned at the top and bottom. The lower coil allows the tank to be charged with thermal energy from an external source (e.g., a heat pump, solar thermal collector). The upper coil, on the other hand, is utilised for DHWT production, facilitating indirect heat transfer between the stored hot water in the tank and the incoming cold mains water. During this process, mains water enters the tank through the lower inlet of the upper coil, interacts thermally with the water inside the tank to increase in temperature, and exits as hot water from the upper outlet. This design approach aims to ensure hygienic DHWT supply while enhancing energy efficiency.

To improve the thermal performance of the tank, the PCM tubes were attached to the coils using clip mechanisms that ensured both the PCM tubes remained in place and efficient heat transfer was ensured. Consequently, the PCM's latent heat storage capacity enhances the tank's energy efficiency through minimising fluctuations in hot water temperature. During heating and cooling processes, the PCM stores energy via phase change (solid-to-liquid transition), helping to maintain the water within the desired temperature range for extended periods. This mechanism is particularly effective in meeting sudden demand, ensuring sufficient hot water is available at a stable temperature.

Figure 1. 300 L domestic hot water tank [16]

2.2 Baseline Experimental Procedure

Charge, discharge, and heat-loss experiments were performed on the conventional DHWT (without PCM) test system, and the resulting data were used to validate the analysis model as reference case. During the charging phase, the storage tank was supplied by a heat pump operating at 50 °C with a volumetric flow rate of 24 L/min. Charging was continued until the tank temperature reached 50 °C.

In the discharging phase, DHWT production was obtained by circulating mains water through the coil at 12.5 °C with a flow rate of 8 L/min. The discharge test was terminated when the temperature measured at the coil outlet dropped below 40 °C.

For the heat-loss tests, the tank temperature was first raised to 55 °C (the maximum temperature attainable by the heat pump). The tank maintained at 55 °C was then left in a stand-by mode under natural convection conditions in accordance with the requirements of the TS EN 12897+A1:2020-03 standard.

2.3 Determination of PCM Properties

The PCM plays a critical role in determining the thermal energy storage capacity and optimising the overall energy efficiency of the tank. In this context, the thermophysical properties of the PCMs were thoroughly examined, and its suitability for the system design was evaluated.

Table 1. Properties of the PCMs [15, 17]

Paraffin based PCM type	RT47	MP46	MP52
Melting Temp. (°C)	48	49.1	54.9
Solidification Temp. (°C)	41	42.5	42.6
Latent heat storage capacity (kJ/kg)	160	214	198.4
Specific Heat Capacity (kJ/kg.K)	2	2.2	2.66
Solid Density (kg/m3)	880	772	808
Fluid Density (kg/m3)	770	750	783
Heat Conduction (W/m.K)	0.2	0.137	0.129

2.4 Determination of PCM Capsule Geometry

Physical and thermal properties of the PCMs, including melting – solidification temperature range, material type, thermal conductivity, density, specific heat, and latent heat capacity were derived from both literature and manufacturer specifications (Table 1). These data were used as input parameters in the CFD analyses, ensuring accurate modelling of the tank's performance during charging, discharging, and standby periods.

The paraffin-based PCMs, with a phase change temperature in the range of 40–50 °C, were selected based on a combination of technical and practical criteria. First, the chosen temperature range aligns with the DHWT requirements. Also, paraffin provides high latent heat capacity and significant enthalpy of solidification per unit temperature during phase change. Additionally, factors such as chemical stability, cycle durability, compatibility with metal containers without causing corrosion, and commercial availability were also considered critical. These properties are vital for long-term stable operation of the system while enhancing energy efficiency.

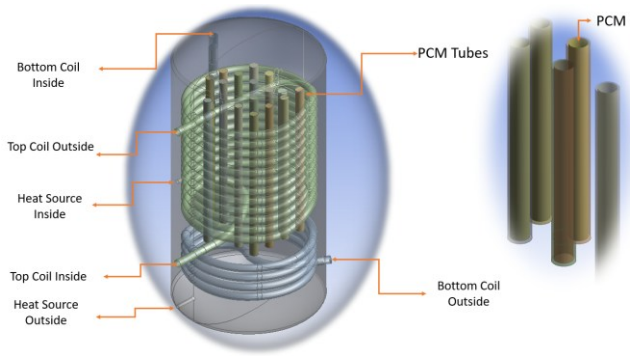

Figure 2. 300 L DHWT with PCM

Table 2. PCM tube details [11]

Material	SAE 304
Length	650 mm
Inside diameter	30 mm
Outside diameter	33.4 mm

The method of integrating PCMs into the DHWT directly affects the thermal performance, particularly in terms of heat transfer surface area. In this study, cylindrical capsules with a relatively higher surface area-to-volume ratio were selected to enhance the heat exchange within the tank (Figure 2) [10]. These cylindrical capsules improve the thermal interaction between the PCM and water due to higher thermal conductivity of the metallic tubes, optimising energy storing and releasing processes and enhancing the overall system efficiency [4].

Capsule diameter is another important factor that has direct impact on the thermal performance of the PCM. Reducing the capsule diameter limits the total heat transfer surface area, which decreases the heat transfer rate. Conversely, excessively increasing the capsule diameter may leave the inner regions of the PCM unmelt. This scenario could result in excessive use of PCM and hinder the tank from delivering hot water at the desired temperature during discharging, negatively impacting system performance. Based on findings from the existing studies in the literature [11], the inner diameter, outer diameter, and length of the PCM tubes were adapted and 12 tubes are used in the system, their specifications are given in Table 2.

In addition to tube dimensions, the placement of PCM capsules within the tank significantly affects thermal performance. In the current design, PCM tubes are positioned vertically at a mid-height between the serpentine and the tank centre. This vertical orientation is chosen to be perpendicular to the upward flow of water due to buoyancy; it enhances convective heat transfer between the PCM capsules and the surrounding water.

The tubes are secured to the serpentines using 37.5 mm clips, resulting in a distance of 54.2 mm from the centre to the serpentine. This configuration ensures uniform spacing and stable flow paths. Careful determination of these size parameters is crucial for enhancing heat transfer while maintaining optimum thermal energy storage. Consequently, capsule geometry and sizing are considered fundamental design factors for improving both energy storage capacity and hot water output performance.

2.5 CFD Modelling

The simulations were governed by the fundamental conservation equations of mass, momentum, and energy. The continuity equation ensures mass balance within the tank, while the momentum equations, formulated as the Reynolds-averaged Navier–Stokes (RANS) equations, account for pressure forces, viscous effects, and buoyancy-driven flow. The energy equation describes transient heat transfer by incorporating both conduction and convection mechanisms, enabling an accurate representation of the thermo-fluid behaviour of the tank during the charging and discharging processes. The fluid flow and thermal behaviour within the tank were evaluated using transient CFD simulations performed in ANSYS Fluent R16.2.

Turbulence effects were modelled using the k–ω turbulence model, a widely adopted two-equation approach in computational fluid dynamics. This model was chosen due to its strong performance in accurately capturing natural and forced convection events under

low to medium Reynolds number conditions. Specifically, the standard k–ω model is better suited for the thermally stratified and mixed convection regimes encountered in the storage tank and provides better handling in the near-wall region and better sensitivity to buoyancy-driven flow structures compared to the k–ε model.

This model resolves two coupled partial differential equations for the turbulence kinetic energy (k) and the specific dissipation rate (ω), where k represents the energy of turbulent velocity fluctuations and ω characterizes the rate at which this energy is dissipated into internal thermal energy.

Mass conservation:

$$\nabla \cdot \vec{V} = 0 \quad (1)$$

Momentum conservation:

$$\rho \frac{\partial \vec{V}}{\partial t} + \rho(\vec{V}\nabla)\vec{V} = -\nabla P + \mu \nabla^2 \vec{V} + \rho\beta\vec{g}\,(T - T_0) + \vec{S} \quad (2)$$

Energy conservation:

$$\frac{\partial}{\partial t}(\rho H) + \nabla \cdot \left(\rho \vec{V} H\right) = \nabla \cdot (k_1 \nabla T) \quad (3)$$

The Darcy source term is used in Eq. (2) due to the porosity change in the soft region [18].

$$\vec{S} = \frac{(1-\lambda)^2}{\lambda^3 + 0.001}\vec{V} A_{mushy} \quad (4)$$

The symbols $V, \rho, P, \beta, t, \mu, g, k_1$ denote velocity, density, pressure, thermal expansion coefficient, time, dynamic viscosity, gravitational acceleration, and thermal conductivity, respectively.

Enthalpy represents the total thermal energy of the PCM and consists of both sensible and latent heat capacities. The sensible heat varies with temperature according to the specific heat capacity, while the latent heat accounts for the energy absorbed or released during phase change at nearly constant temperature. In CFD-based PCM modelling, the enthalpy formulation enables accurate tracking of melting and solidification by coupling temperature-dependent sensible heat with the latent heat source term. This approach ensures a consistent and energy-conserving representation of the phase change process across the computational domain.

$$H = h + \Delta H \quad (5)$$

The sensible heat:

$$h = h_0 + \int_{T_0}^{T} C_p dT \quad (6)$$

The latent heat:

$$\Delta H = \lambda L$$

L is the latent heat of the PCM. λ is the liquid fraction in the soft region, with values between 0 and 1.

$$\lambda = \begin{cases} 0 & T < T_{solid} \\ \frac{T - T_{solid}}{T_{liquid} - T_{solid}} & T_{solid} < T < T_{liquid} \\ 1 & T > T_{liquid} \end{cases} \quad (7)$$

The phase change process in the PCM was modelled based on the classical enthalpy–porosity approach. In this method, the phase transition is defined by accounting for enthalpy variations during the solid-to-liquid transition, and energy transfer within this region is computed [12, 13]. This approach allows the latent heat storage capacity of the PCM and its impact on the overall thermal performance of the tank to be numerically simulated.

2.5.1 Mesh Structure

A locally refined mesh was generated over the geometric model in critical regions. In particular, smaller cell sizes were applied at the coil surfaces, around the PCM tubes, and at the fluid inlet and outlet zones to ensure detailed resolution. This strategy enables accurate modelling of both flow and heat transfer behaviour. The mesh details are presented in Table 3, demonstrating that the simulations are sufficiently stable and resolved numerically (Figure 3, Figure 4). This configuration allows for precise investigation of both energy storage and DHWT supply processes.

A total of 10 iterations were conducted during the simulation process, and the time step size was set to 0.1 s, resulting in a CFL number of 2.66. The primary reason for choosing a time step of 0.1 was to increase temporal resolution while maintaining a stable CFL value within

acceptable limits for incompressible flow, thereby improving the accuracy of the CFD predictions and enabling a more precise representation of transient flow structures, temperature gradients, and convection-driven circulation patterns inside the tank. However, although more precise results were obtained setting time step at 0.1 s has increased the duration tenfold.

Table 3. Model mesh quality values

Element number	1,347,048
Skewness value (max)	0.78
Orthogonal Quality (min)	0.23
Aspect Ratio value (max)	10.6

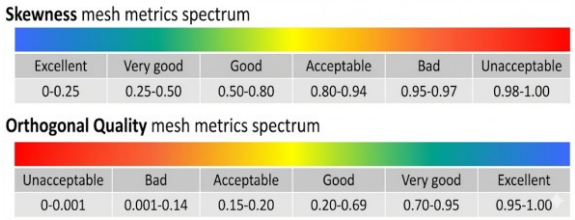

Figure 3. Mesh quality metric

The numerical configuration applied in the transient analyses was as follows:

- Pressure–velocity coupling: SIMPLE
- Time step: 0.1 s
- Courant number: 2.66
- Boundary layer thickness: 0.5 mm
- Convergence criteria: 10^{-5} for continuity and momentum, 10^{-6} for energy
- Under-relaxation factors: default settings (energy=1.0)

Within the framework of the RANS equations, the eddy viscosity ν_T is defined as the ratio of the turbulence kinetic energy to the specific dissipation rate, i.e., $\nu_T = k/\omega$. The transport equations governing the temporal and spatial evolution of the turbulence kinetic energy k and the specific dissipation rate ω are given as follows [19]:

$$\frac{\partial(\rho k)}{\partial t} + \frac{\partial(\rho u_j k)}{\partial x_j} = \rho P - \beta^* \rho \omega k + \frac{\partial}{\partial x_j}\left[\left(\mu + \sigma_k \frac{\rho k}{\omega}\right)\frac{\partial k}{\partial x_j}\right], with\ P = \tau_{ij}\frac{\partial u_i}{\partial x_j} \quad (8)$$

$$\frac{\partial(\rho w)}{\partial t} + \frac{\partial(\rho u_j w)}{\partial x_j} = \frac{\alpha\omega}{k}\rho P - \beta\rho\omega^2 + \frac{\partial}{\partial x_j}\left[\left(\mu + \sigma_k \frac{\rho k}{\omega}\right)\frac{\partial \omega}{\partial x_j}\right] + \frac{\rho\sigma_d}{\omega}\frac{\partial k}{\partial x_j}\frac{\partial \omega}{\partial x_j} \quad (9)$$

The symbols $k, \omega, u_i, u_j, x_i, x_j$ denote Favre-averaged specific turbulence kinetic energy, specific dissipation rate, Favre-averaged velocity vectors (u values), and position vectors (x values), respectively.

2.5.2 Tank Charging Simulation Procedure

For the charging process, both the PCM-integrated and conventional (water based) DHWTs were initially filled with water at a uniform temperature of 12.5 °C. The heating process was simulated to reflect realistic operating conditions, using a heat pump with an outlet temperature of 50 °C at a flow rate of 24 L/min. Firstly, the charging behaviour of the conventional tank was analysed, and the resulting temperature distributions and thermal response were validated against experimental data. This validation ensured the reliability of the simulation model and provided a basis for analysing the PCM-integrated tank.

The melting process of the PCM was specifically accounted for in the simulations, as it directly affects heat transfer within the tank and plays a critical role in determining the charging time. During phase change, the PCM stores latent heat, slowing the temperature rise of the

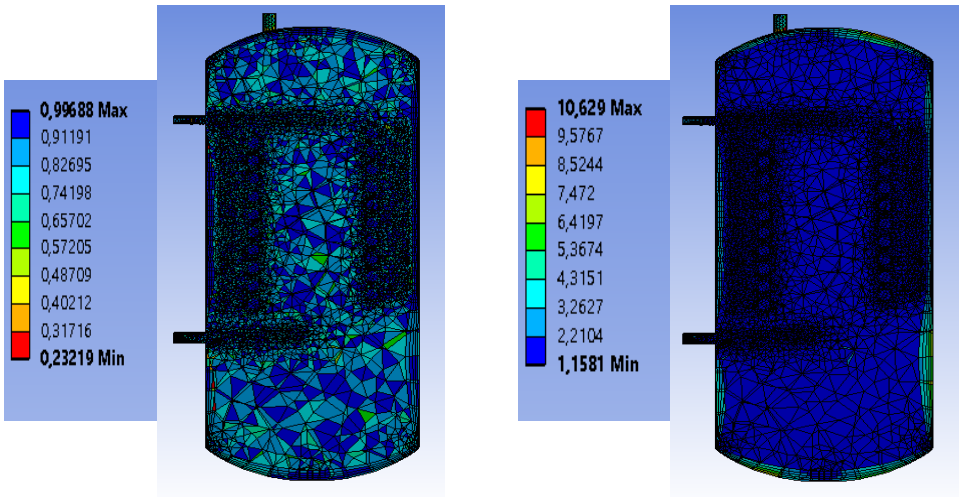

a b

Figure 4. a) Orthogonal quality, b) Aspect ratio views

water and helping maintain thermal homogeneity within the tank. In both tank configurations, the charging process was terminated once the average water temperature reached 50 °C. This approach allowed for a consistent comparison of the thermal effects and energy storage capacity of the PCM with experimental conditions.
This methodology has enabled a detailed assessment of the effects of PCM integration on tank charging time, energy storage efficiency, and hot water output.

2.5.3 Tank Discharging Simulation Procedure

The discharge process was conducted to evaluate the thermal response behaviour of the tanks, which had initially reached an average temperature of 50 °C at the end of the charging phase. For the discharge analysis, both the PCM-integrated and conventional tank were defined with a uniform temperature of 50 °C. Subsequently, mains water at 12.5 °C was supplied to the coil inlet at a constant flow rate of 8 L/min. This scenario simulates real operational conditions of the DHWT consumption.

During the discharge process, the cold water circulating through the coil indirectly transferred heat to the water in the tank, producing usable hot water. As the tank temperature decreased, solidification occurred in the PCM; the molten paraffin solidified, releasing latent heat. This helped maintain the water within the desired temperature range for a longer duration and demonstrated how the energy storage capacity of the PCM stabilizes tank performance during discharge.

The discharge process halted once the outlet temperature of the DHWT dropped below 40 °C. This set temperature was defined as a practical comfort limit and ensured the comparability of the analyses. Temperature distributions, outlet temperature–time profiles, and internal heat transfer data obtained during the discharge period were used to assess the effects of PCM on thermal stability and energy efficiency.

2.5.4 Heat Loss Simulation Procedure

The heat loss analysis was carried out in accordance with the TS EN 12897+A1:2020-03 standard and was designed to evaluate the energy losses occurring when the domestic DHWT tank is left idle for a certain period after the charging process. Within this scope, both the PCM-integrated and conventional tank models were simulated for 180 minutes after the average water temperature reached 55 °C [7, 14].

During the analysis, the tank's inlet and outlet were closed to create a static system, and heat transfer between the tank surface and the environment was limited to natural convection

and surface radiation. No active cooling or additional heating was applied, and the ambient temperature was set to a constant 20 °C in accordance with the TS EN 12897 standard and maintained throughout the simulation.

The tank insulation was modelled based on commonly used polyurethane foam insulation properties, and heat transfer from the tank surface to the surroundings was calculated according to the thermophysical properties of this material. In the PCM-integrated tank, the latent heat storage capacity of the paraffin-based phase change material, near its melting temperature, was utilized to delay the temperature drop and enhance the thermal stability of the tank during the idle period. This approach allowed for a numerical assessment of the effects of PCM on energy storage and heat loss.

3. Results and Discussion

3.1 Charging Process Analysis Results

The charging simulations were carried out by initially setting both the PCM-integrated and conventional tanks to a uniform water temperature of 12.5 °C. A heat pump supplying 50 °C water at a flow rate of 24 L/min was used to evaluate the temperature evolution and charging dynamics. The temperature fields obtained for the conventional and PCM-integrated configurations at their respective charging durations are presented in Figure 4.

To determine the effect of phase change materials on overall thermal performance, PCM temperature variations and corresponding melting rates were evaluated comparatively. Figure 5 shows: (a) initial tank temperature, (b) temperature range of the conventional tank at the end of the charging time (100 min), and (c-e) temperature distributions of the RT47, MP46, and MP52 integrated tanks at their respective charging times (105, 110, and 105 min).

According to Table 4, the simulated charging time of the conventional tank (100 min) showed strong agreement with experimental measurements. Under the same operating conditions, the melting fractions of the integrated PCMs at 105 min were 90 % for RT47, 88 % for MP46, and 75 % for MP52. These results confirm that PCM addition increases the tank's thermal storage capacity without altering the fundamental charging behaviour.

Although the RT47 and MP46 samples required approximately 140 min to reach complete melting, the majority of their latent heat potential had already been activated within the effective charging window. The remaining unmelted fraction did not cause operational delay or degradation in charging performance. Therefore, PCM integration can be considered an effective enhancement strategy that increases storage density while maintaining comparable charging times to the baseline configuration.

Table 4. Test vs simulation charge results

Method (24 L/min)	Charge Temp. (°C)	Charging Time (min)	Diff. (%)	Melting Time (min)
Water (Exp.)	50	100	-	-
Water (Sim.)	50	100	-	-
RT47	50	105	5	105
MP46	50	105	10	110
MP52	50	105	-	105 (75%)

3.2 Discharging Process Analysis Results

During the discharging simulations, mains water at 12.5 °C and 8 L/min was circulated through the upper coil of tanks initially at an average temperature of 50 °C. The process was terminated once the outlet temperature dropped below the comfort threshold of 40 °C. Figure 5 presents the temperature distributions for both the conventional and PCM-integrated tanks at the end of their respective discharge durations.

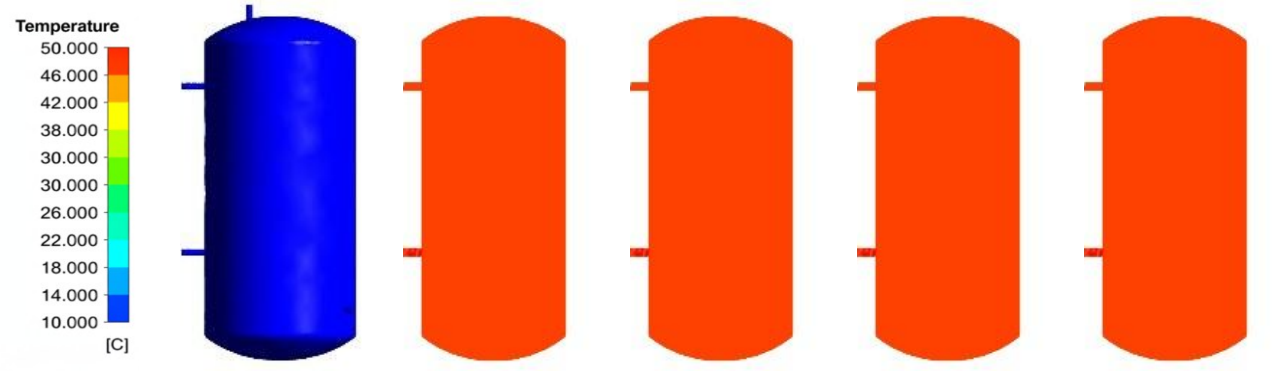

0.min ≈ 12.5˚C a | 100.min ≈ 50˚C b | 105.min ≈ 50˚C c | 110.min ≈ 50˚C d | 105.min ≈ 50˚C e

Figure 5. Standard vs PCMs charging time

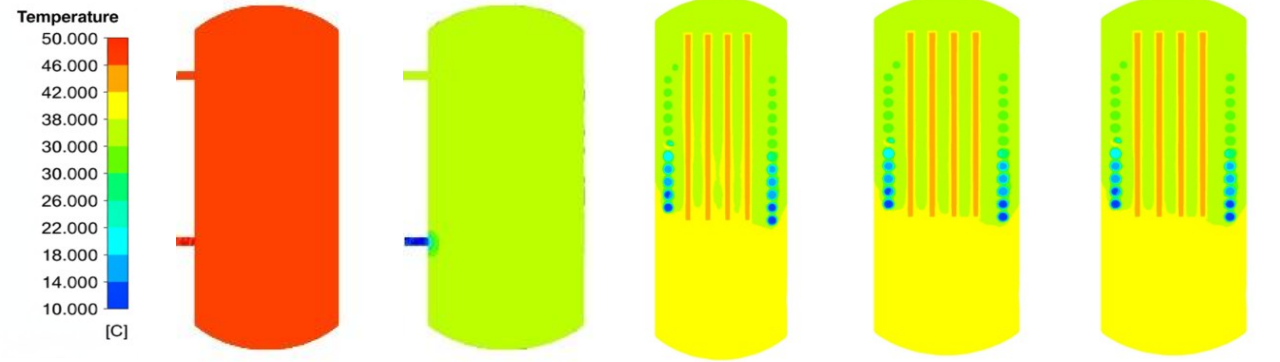

0.min ≈ 50˚C a | 14.10 min ≈ 40˚C b | 16.40 min ≈ 40˚C c | 16.20 min ≈ 40˚C d | 15.30 min ≈ 40˚C e

Figure 6. Standard vs PCMs discharging time

Figure 6 presents: (a) the initial temperature distribution within the tank, (b) the temperature field of the conventional tank at the end of the discharge period (14.10 min), and (c–e) the temperature distributions of the RT47, MP46, and MP52-integrated tanks corresponding to their respective discharge durations (16.40, 16.20, and 15.30 min).

As summarised in Table 5, the simulated discharge time of the conventional tank (14.10 min) closely matched experimental findings.

The RT47, MP46, and MP52-integrated tanks exhibited longer discharge durations of 16.40, 16.20, and 15.30 min, respectively. These increments correspond to approximately 20, 16, and 10 additional litres of usable hot water compared with the reference case.

The extended discharge periods result from the gradual release of latent heat during PCM solidification. As the tank cools, the PCMs transfer stored thermal energy back to the surrounding water, moderating temperature decay and sustaining the outlet temperature above 40 °C. This mechanism enhances the effective hot water volume and contributes to improved thermal efficiency during draw-off periods.

3.3 Heat Loss Analysis Results

Heat loss performance was evaluated according to the TS EN 12897+A1:2020-03 standard. This evaluation was carried out by initially maintaining the average temperature of both conventional and PCM integrated tanks at 55 °C and then applying a 180-minute standby period without water circulation. The

ambient temperature was kept constant at 20 °C, and heat transfer was achieved through natural convection and surface radiation. Figure 6 shows the average temperatures of the tanks at the end of the 180-minute holding period.

Figure 7 shows: (a) the initial temperature of the tank, (b) the temperature distribution of the conventional tank at the end of 180 minutes of analysis, and (c-e) the temperature distribution of the PCM-integrated tanks (RT47, MP46, and MP52) at the end of the same period.

Table 6 indicates that the conventional tank exhibited a heat loss of approximately 86.9 W, consistent with experimental observations. The PCM-integrated tanks demonstrated reduced heat losses of 82.3 W (RT47), 82.24 W (MP46), and 79.95 W (MP52), confirming an improvement in thermal retention.

This enhancement is attributed to the latent heat buffering capacity of the PCMs near their phase change temperatures. As the stored energy is gradually released during cooling, the rate of temperature decay decreases, leading to lower static heat losses and improved standby efficiency. Overall, the integration of PCMs not only increases usable hot water availability but also enhances energy performance by reducing heat losses during no-load conditions.

Table 5. Test vs simulation discharge results

Method (8 L/min)	Discharge Temp. (°C)	Discharge Time (min. s)	Diff. (%)	HW Amount (L)
Water (Exp.)	50	14.10	-	113
Water (Sim.)	50	14.10	-	113
RT47	50	16.40	20	133
MP46	50	16.20	18	132
MP52	50	15.30	9.42	126

Table 6. Test vs simulation heat loss results

Method (Natural Convection)	Heat Loss Temp. (°C)	Heat Loss Time (hour)	Heat Loss (W)	Diff. (%)
Water (Exp.)	55	3	92.7	-5.75
Water (Sim.)	55	3	86.9	-
RT47	55	3	82.3	5.35
MP46	55	3	82.2	5.36
MP52	55	3	79.9	7.99

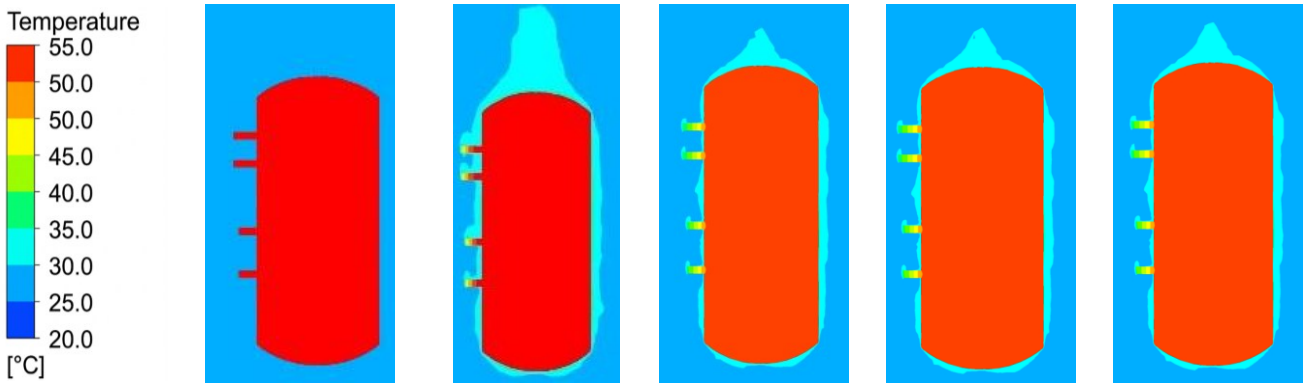

Figure 7. Standard vs PCMs heat loss time

4. Conclusions

This study numerically evaluated the thermal performance of a 300 L DHWT integrated with 3 kg of paraffin-based PCMs under charging, discharging, and standby conditions, and compared the results with those of a conventional configuration. CFD

simulations showed that PCM integration had a negligible influence on charging behaviour. The conventional tank reached 50 °C in 100 minutes, whereas the RT47-integrated tank achieved the same temperature in 105 minutes, indicating only a minor increase of approximately 5 %.

In contrast, PCM incorporation significantly enhanced discharging performance. The useful hot water delivery period of the conventional tank (14.10 min) was extended to 16.40 min with RT47, corresponding to an additional 20 L of water above the comfort threshold. This improvement arises from the latent heat released during solidification, which effectively stabilizes outlet temperature during periods of decreasing tank temperature.

Standby heat-loss analyses conducted in accordance with TS EN 12897+A1:2020 highlighted further thermal advantages. The MP52-integrated tank exhibited a heat loss of 79.95 W after 180 minutes, compared with 86.9 W for the conventional system, confirming superior temperature retention through latent heat buffering.

Among the tested PCMs, RT47 and MP46 demonstrated the most favourable overall performance due to their melting ranges (40–55 °C) aligning well with DHWT operating temperatures and enabling efficient charge–discharge behaviour. Although MP52 contributed less to discharge extension, it performed best in reducing standby heat losses.

Overall, integrating a small PCM quantity (~3 kg) into a 300 L DHWT provides measurable performance gains—extending hot water availability, improving thermal stability, and reducing standby losses—while maintaining comparable charging times. These outcomes indicate that PCM-integrated storage tanks offer a practical and effective pathway for improving energy efficiency in DHWT applications.

Future work will focus on the experimental validation of PCM-integrated hot water tanks under realistic domestic water usage conditions. Furthermore, investigating advanced serpentine and PCM encapsulation techniques in different tank geometries could further enhance heat transfer performance. Moreover, comprehensive studies on the effects of varying PCM quantities and incorporating these findings into energy class assessment procedures could support the development of more efficient storage tank designs.

Acknowledgements

This study was carried out within the framework of project number 3248224, supported by the TÜBİTAK 1832 Green Transformation in Industry Call. We would like to thank the project partners Solimpeks Energy Industry and Trade Inc., Innorma R&D Inc., and Petroyag and Chemicals Industry and Trade Inc. for their valuable contributions throughout the project process.

References

[1] IEA (2023), *Energy Efficiency 2023, IEA, Paris* https://www.iea.org/reports/energy-efficiency-2023, Licence: CC BY 4.0

[2] Energy Performance of Buildings Directive, 2024, Energy Performance of Buildings Directive

[3] Liang, H., Niu, J., & Gan, Y. (2020). Performance optimization for shell-and-tube PCM thermal energy storage. *Journal of Energy Storage*, *30*. https://doi.org/10.1016/j.est.2020.101421

[4] Erdemir, D. (2020). Kapsüllenmiş Faz Değiştiren Malzemelerin Sıcak Su Tankları İçerisindeki Konumlarının Isıl Enerji Depolama Performansı Üzerindeki Etkisi. Erciyes Üniversitesi Fen Bilimleri Enstitüsü Fen Bilimleri Dergisi, 35(3), 24-33.

[5] Erdemir, D., & Altuntop, N., (2019). Experimental Investigation of Phase Change Material Utilization Inside the Horizontal Mantled Hot Water Tank (Accepted Paper). *International Journal Of Exergy* , vol.1, 1-28. https://dx.doi.org/10.1504/IJEX.2020.104722

[6] Erdemir, D., Ozbekler, A., & Altuntop, N. (2022). Experimental investigation on the effect of the ratio of tank volume to total capsulized paraffin volume on hot water output for a mantled hot water tank. *Solar Energy*, *239*, 294–306. https://doi.org/10.1016/j.solener.2022.05.010

[7] Junga, R., Pospolita, J., Kabaciński, M., Sobek, S., Stanisławski, R., Mami, M. A., … Mruk, Z. (2024). Numerical modeling of heat losses from hot water storage tank. *Case Studies in Thermal Engineering*, *62*. https://doi.org/10.1016/j.csite.2024.105146

[8] Yildirim N., Kahraman I. & Umdu E., (2023) Exergetic Performance Assessment of Different Building Heating Systems https://doi.org/10.5281/zenodo.7487556

[9] M. S. Büker, V. C. Güran, A. E. Onay ve H. İ. Dağ, "Thermal performance assessment and energy efficiency improvement of a domestic hot water tank with PCM," in Proc. ULIBTK'25 Uluslararası Katılımlı 25. Isı Bilimi ve Tekniği Kongresi, Adana, Türkiye, 10-12 Eylül 2025, pp. 977-983.

[10] Koželj, R., Mlakar, U., Zavrl, E., Stritih, U., & Stropnik, R. (2021). An experimental and numerical analysis of an improved thermal storage tank with encapsulated PCM for use in retrofitted buildings for heating. *Energy and Buildings*, *248*. https://doi.org/10.1016/j.enbuild.2021.111196

[11] Najafian, A., Haghighat, F., & Moreau, A. (2015). Integration of PCM in domestic hot water tanks: Optimization for shifting peak demand. *Energy and Buildings*, *106*, 59–64. https://doi.org/10.1016/j.enbuild.2015.05.036

[12] Belhadad, T., Draoui, B., & Bouabdallah, S. (2023). CFD investigation of fin design influence on phase change using ANSYS Fluent enthalpy-porosity method. *Journal of Energy Storage, 62*, 107361. https://doi.org/10.1016/j.prime.2023.100306

[13] Saliby, A., Hammami, A., & Sadok, D. (2024). Experimentally based testing of the enthalpy-porosity method for the numerical simulation of phase change of paraffin-type PCMs. *Journal of Building Engineering, 85*, 108467. https://doi.org/10.1016/j.est.2023.107876

[14] TS EN 12897+A1, 2020, *Su temini - Dolaylı olarak ısıtılan havalandırmasız (kapalı) ısıtıcılı su depoları için özellikler,* Standard Detayı

[15] Rubitherm, Rubitherm Technologies GmbH, https://www.rubitherm.eu/produktkategorie/organische-pcm-rt (accessed Nov. 18, 2025).

[16] Solimpeks, "Solikombi 300 Hijyenik Boyler - Serpantinli - Akümülasyon tankı - boiler," Solimpeks Güneş Enerjisi Sistemleri | Isı Pompası - Fotovoltaik Panel - Boyler - Solar Enerji, https://www.solimpeks.com.tr/urun/solikombi-300-hijyenik-boyler/ (accessed Nov. 18, 2025).

[17] Petroyağ, "Endüstriyel Yağlar: Petroyağ ürünler," Endüstriyel Yağlar | Petroyağ Ürünler, https://www.petroyag.com/urunler (accessed Nov. 18, 2025).

[18] A. D. Brent, V. R. Voller, and K. J. Reid, "Enthalpy-porosity technique for modeling convection-diffusion phase change: Application to the melting of a pure metal," Numerical Heat Transfer, vol. 13, no. 3, pp. 297–318, Apr. 1988. doi:10.1080/10407788808913615

[19] Wilcox, D. C. (2008), "Formulation of the k–ω Turbulence Model Revisited", *AIAA Journal*, **46** (11): 2823–2838, Bibcode:2008AIAAJ..46.2823W, doi:10.2514/1.36541